

# Observational Evidence for Rising Penumbra Flux Tubes?

J. Jurčák · M. Sobotka

Received: 1 December 2006 / Accepted: 28 February 2007 /  
Published online: 17 April 2007  
© Springer 2007

**Abstract** On 13 May 2000 parts of a penumbra were observed in an active region NOAA 8990 with the La Palma Stokes Polarimeter attached to the Swedish Vacuum Solar Telescope. The stratification over the solar atmosphere of different physical parameters is retrieved from these data by using the Stokes inversion based on response functions. The results confirm the previous findings of the penumbral structure. In general, the magnetic field becomes weaker and more horizontal with increasing distance from the umbra and the line-of-sight velocities are increasing towards the outer boundary of the penumbra. The results also suggest the existence of the unresolved fine structure of the penumbra. The stratifications of the temperature and of the magnetic field strength indicate the presence of rising flux tubes, which were predicted theoretically by Schlichenmaier, Jahn and Schmidt (1998, *Astron. Astrophys.* **337**, 897).

**Keywords** Sun: sunspots · Sun: magnetic field

## 1. Introduction

Despite prolonged interest in sunspot penumbrae and corresponding amount of analyses, there is still a lack of confirmed facts regarding the penumbral fine structure. However, the global properties of the plasma quantities in the penumbra are well known. The magnetic field strength is decreasing outwards with no detectable jump on the umbral-penumbral boundary. The magnetic field is almost vertical in the umbral parts of the sunspot and becomes horizontal at the outer boundary of the penumbra, creating a magnetic canopy above the surrounding area (see the review by Solanki, 2003, and references therein). The penumbral velocities are composed mostly of the Evershed flow, which is almost horizontal and is pointing outwards at photospheric heights. The magnitude of the velocity increases

---

J. Jurčák (✉) · M. Sobotka  
Astronomical Institute, Academy of Sciences of the Czech Republic, 25165 Ondřejov,  
Czech Republic  
e-mail: jurcak@asu.cas.cz

from the inner parts of the penumbra to its outer edge (Solanki, 2003; Borrero *et al.*, 2004; Bellot Rubio, Schlichenmaier, and Tritschler, 2006).

The magnetic fine structure of the penumbra was for the first time studied by Beckers and Schröter (1969), who found stronger and more vertical magnetic field in dark filaments. Note that the vertical direction corresponds to zero value of inclination in our notation and thus the less and more inclined field correspond to more vertical and more horizontal magnetic field, respectively.

The horizontally oriented Evershed flow points to the existence of structures that must have horizontal magnetic field, as the flow follows the magnetic field lines. Recently, many authors agreed on the uncombed structure of the penumbral magnetic field, which was proposed by Solanki and Montavon (1993) to explain the broad-band circular polarization of sunspots and further developed by Martínez Pillet (2000) and recently by Müller *et al.* (2007). This uncombed structure is created from horizontal flux tubes embedded in a more vertical and stronger background field. Evidence for this empirical model were found in recent analyses of observations (see *e.g.* Borrero *et al.*, 2004, 2006; Bellot Rubio, Balthasar, and Collados, 2004; Bellot Rubio, Schlichenmaier, and Tritschler, 2006; Langhans *et al.*, 2005). This configuration can also explain the horizontality of the Evershed flow if this one is carried by the flux tubes as suggested by the aforementioned observational analyses.

Except for the analysis by Langhans *et al.* (2005), the conclusions are based on the inversion of the observed Stokes profiles. The spatial resolution of this kind of observation is lower than the resolution of magnetograms and Dopplergrams obtained with the 1-m Solar Telescope used by Langhans *et al.* (2005), who resolved directly the polarization signal of the horizontal magnetic flux tube and its surroundings with a spatial resolution of about  $0.2''$ . The best spectropolarimetric observations reach a spatial resolution of around  $0.5''$ , which is insufficient for distinguishing the penumbral fine structure as even at a resolution of  $0.1''$  some of the filaments remain unresolved (Roupe van der Voort *et al.*, 2004).

Thus it seems necessary to perform the inversion with a two-component model atmosphere. However, Borrero *et al.* (2004) showed the possibility of resolving the uncombed structure of the penumbra even with a one-component model atmosphere. This approach is used in our analysis of the data obtained with the La Palma Stokes Polarimeter (LPSP) attached to the Swedish Vacuum Solar Telescope (SVST), which are described in Section 2 along with the description of the inversion code. In Section 3 we briefly describe the general results, but the main part is devoted to the analysis of the fine structure of the penumbral filaments.

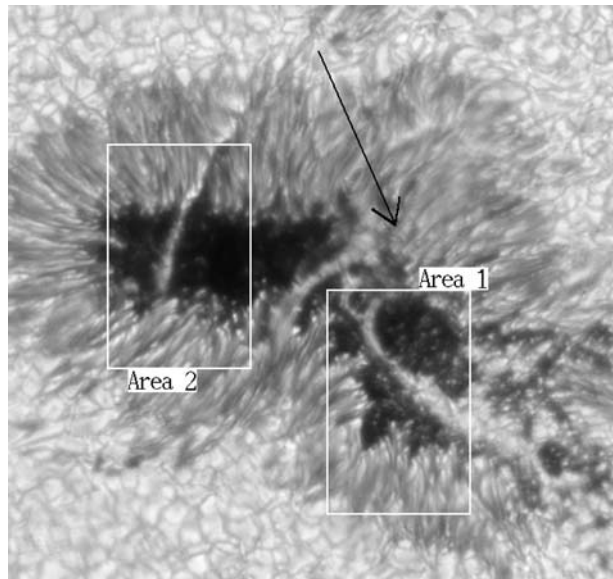
## 2. Observations and Data Processing

### 2.1. Observations

On 13 May 2000, an irregular leading sunspot in the active region NOAA 8990 was observed with LPSP (Martínez Pillet, Collados, and Sánchez Almeida, 1999) attached to the spectrograph of the 0.5-m SVST, La Palma (Scharmer *et al.*, 1985). The spot was located near the disc center, at heliocentric position  $14^\circ$  N and  $17^\circ$  W (heliocentric angle  $\mu = 0.907$ ).

The white-light image of this active region is shown in Figure 1. Two areas (1, 2) marked in Figure 1 were scanned in the magnetically sensitive lines Fe I 630.15 nm (Landé factor  $g = 1.67$ ) and Fe I 630.25 nm ( $g = 2.5$ ). These two maps were taken at 9:03 and 9:13 UT.

**Figure 1** White-light image of the leading sunspot in NOAA 8990 with the marked areas under study. The arrow points to the north direction.



The pixel size of the spectropolarimetric camera was  $0.078''$ . The width of the spectrograph slit was equivalent to  $0.32''$  and the scanning step was  $0.24''$ . The resulting spatial resolution, including the effect of seeing, was about  $0.7''$  for the spectropolarimetric observations. The exposure time for one position of the spectrograph slit was 3 s, in which all Stokes profiles ( $I$ ,  $Q$ ,  $U$ , and  $V$ ) were acquired. The zero of velocity was determined by using the telluric line in the red wing of the Fe I 630.25 nm line. Other details about the observation can be found in Jurčák, Martínez Pillet, and Sobotka (2006) or Jurčák (2006).<sup>1</sup>

## 2.2. Inversion Method

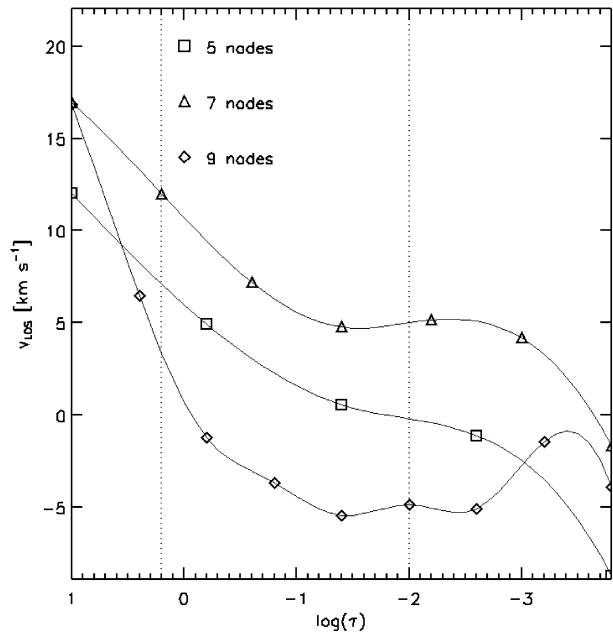
We used the inversion code SIR (Stokes Inversion based on Response functions) developed at the Instituto de Astrofísica de Canarias (Ruiz Cobo and del Toro Iniesta, 1992). This code works under the assumption of local thermodynamic equilibrium (LTE) and hydrostatic equilibrium. See the survey studies by Ruiz Cobo (1998) and Westendorp Plaza *et al.* (1998, 2001a).

The inversion code SIR computes the synthetic Stokes profiles by solving the radiative transfer equation for polarized light in a one- or two-component model atmosphere. A non-linear, least-square Marquardt's algorithm (Press, Flannery, and Teukolsky, 1986) is used to modify the parameters of an initial model until the difference between the observed and synthetic Stokes profiles (merit function) is minimized. Bellot Rubio (1999) has shown that the error of the plasma parameter is proportional to the merit function and to the inverse of the response function; therefore, poor fits have larger errors, and parameters that have little influence on the emergent intensity show the largest uncertainties.

The SIR code uses a predefined stray-light profile to fit the observed profiles better. We used the stray-light profile coming from the quiet sun (*i.e.* no stray light in  $Q$ ,  $U$ , and  $V$ ).

<sup>1</sup> Some of the contents of the paper are part of the Ph.D. thesis of the first author. This can be downloaded at [http://www.asu.cas.cz/~sdsa/jurcak\\_en.html](http://www.asu.cas.cz/~sdsa/jurcak_en.html).

**Figure 2** The stratifications of velocity computed with different number of nodes for the same set of Stokes profiles. For display purposes the stratifications obtained with seven and nine nodes are shifted by values of  $+5 \text{ km s}^{-1}$  and  $-5 \text{ km s}^{-1}$ , respectively.



The inversion code returns the stratification of the temperature ( $T$ ), the magnetic field strength ( $B$ ), inclination ( $\gamma_{\text{LOS}}$ ), azimuth ( $\psi_{\text{LOS}}$ ), and the line-of-sight velocity ( $v_{\text{LOS}}$ ), along with the macro- and micro-turbulent velocities, electron pressure, gas pressure, density, and the fraction of the stray light. The transverse-field component direction is unsigned, so that there is a  $180^\circ$  ambiguity in azimuth values. In each of the analysed areas, the sum of differences between the azimuths was minimized, and thus the ambiguity problem was solved. The corrected values of azimuth along with inclination of the magnetic field coming from the SIR code are evaluated with respect to the line of sight. We transformed these variables to the local reference frame; hereafter, the inclination ( $\gamma$ ) is the angle between the magnetic field vector and the local normal line, and the azimuth ( $\psi$ ) is reckoned from the north and increases counterclockwise.

### 2.3. Number of Nodes

The values of plasma parameters are not computed at all optical depths of the model, but only at few grid points called nodes. At remaining depths, they are approximated by the cubic-spline interpolation between the equidistantly distributed nodes. The chosen number of nodes corresponds to the expected complexity of the stratification of the appropriate plasma parameter, *i.e.* one node means that the parameter is height independent, two nodes mean linear dependency with height, and so on.

In Figure 2 are shown the stratifications of line-of-sight (LOS) velocity computed with different number of nodes. The heights of the nodes are marked by various symbols. The dotted lines enclose a region of heights, where the resulting values of plasma parameters are trustworthy and will be discussed in the following sections. The increasing complexity of the LOS velocity stratification with increasing number of nodes in the studied region of heights is apparent.

**Table 1** The numbers of nodes in two different settings of the inversion process.

	Temperature	Mag. field strength	Inclination	LOS velocity
Inversion 1	9	7	5	5
Inversion 2	9	9	9	9

The theoretical predictions (Schlichenmaier, Jahn, and Schmidt, 1998) determine both the location and the diameter of the rising flux tube. Thus we know that the possible presence of the flux tube would be detected in the stratifications of the plasma parameters only if we would have at least three nodes in the studied range of heights, *i.e.* at least seven nodes altogether (as shown in Figure 2).

In Section 3.1 we compare results coming from two different settings of the numbers of nodes. The numbers of nodes are listed in Table 1 for the analysed plasma parameters. In the first run of inversions we used sufficient number of nodes to fit the observed profiles without problems and we are using them here for comparison with the second run of inversions, which has the capability of detecting the eventual flux tubes. Although seven nodes for the plasma parameters should be enough to reveal the expected flux tubes, the results were very similar to the stratifications achieved with fewer nodes and an additional increase in number of nodes was necessary.

Unfortunately, increasing the numbers of nodes increases the number of degrees of freedom. Therefore, the inversion process can minimize the merit function to similar values in several different ways with different resulting stratifications of plasma parameters. The only way to validate the results is by using the continuity of the results and comparing with results with fewer degrees of freedom.

### 3. Results

The obtained results, displayed in Figure 3, are in general in good agreement with previous studies of the penumbral structure (*e.g.* Westendorp Plaza *et al.*, 2001a, 2001b; Langhans *et al.*, 2005; Bellot Rubio, Schlichenmaier, and Tritschler, 2006; Borrero *et al.*, 2006). The magnetic field strength is decreasing with increasing distance from the umbra and becomes more horizontal or even dives back to the sun at some regions far from the umbra. The LOS velocity increases with increasing inclination, *i.e.* towards the penumbra-quiet sun boundary.

The correlations between the continuum intensity and various plasma parameters are unknown; the results are very confusing and contradict each other (see Solanki, 2003). The reason for this can be explained by the argument suggested by Schlichenmaier, Jahn, and Schmidt (1998), *i.e.* the dark parts of the penumbra consist of at least two components with completely different plasma behavior—a background component with a strong magnetic field and a darkened tail of the bright filament with a weak and horizontal magnetic field. Thus the clear correspondence is found only between the continuum intensity and the temperature. In agreement with older studies (Beckers and Schröter, 1969; Wiehr, 2000) and in contrast to recent analyses (Westendorp Plaza *et al.*, 2001a; Langhans *et al.*, 2005), weaker magnetic field is found in brighter areas. The strongest anticorrelation (correlation coefficient of  $-0.5$ ) between these two plasma quantities is found in the discward part of the penumbra in the second area, which is on average the closest one to the umbra, and thus the dark parts there correspond mostly to the background component,

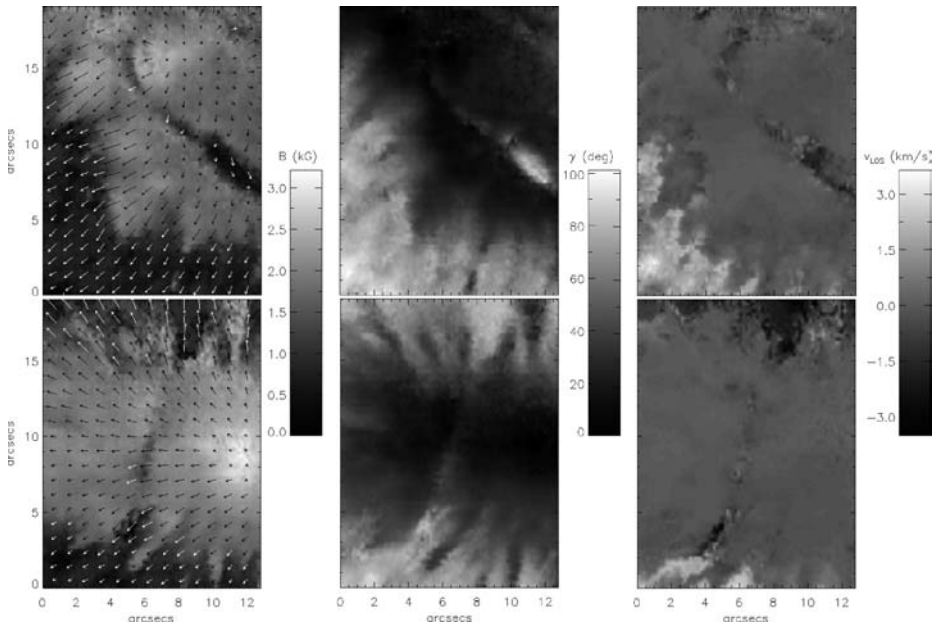


**Figure 3** The resulting maps of magnetic field strength with arrows indicating the azimuth (left column), inclination (middle column), and LOS velocity (right column) in the first and second area (upper and lower rows, respectively) at the optical depth  $\log \tau = -1$ . The resulting maps of plasma parameters from the first run of inversions were used for this purpose.

where the magnetic field is strong, and not to the darkened tails of the bright filaments with reduced magnetic field.

The correlation between the LOS velocity and the magnetic field inclination confirms the results obtained for the first time by Westendorp Plaza *et al.* (2001b), *i.e.* the fastest flows are found in regions where the field lines are diving back towards the solar surface. The anticorrelation between the magnetic field strength and the inclination (*i.e.* weaker fields are more horizontal) confirms the uncombed configuration of the penumbral magnetic field. For more details see Jurčák (2006).

### 3.1. Rising Flux Tubes?

To find evidence for rising flux tubes, we follow the theory according to which the bright grains in the penumbra are places where the flux tubes emerge above the  $\log \tau = 0$  surface. Therefore, we made several vertical cuts through the bright grains in the penumbra. The positions of the cuts are marked in Figure 4 by the inclined arrows starting in the umbra (white arrows) and ending at the edge of the scanned area (black arrows). The vertical and horizontal arrows in Figure 4 enclose the bright grains and correspond to the dashed black lines in Figures 5, 6, and 7, where the stratifications of plasma parameters along the cuts are shown. The solid black lines in the temperature stratifications (Figures 5–7, upper row) correspond to the continuum intensity along the cut. The difference between the right and left columns in Figures 5–7 is in the different numbers of nodes (see Table 1), where the right and left columns correspond to inversion 1 and inversion 2, respectively.

In the upper row of Figure 5 the temperature stratifications along the cut show an elevated filamentary structure hotter than the surrounding plasma, which is rapidly cooled down and

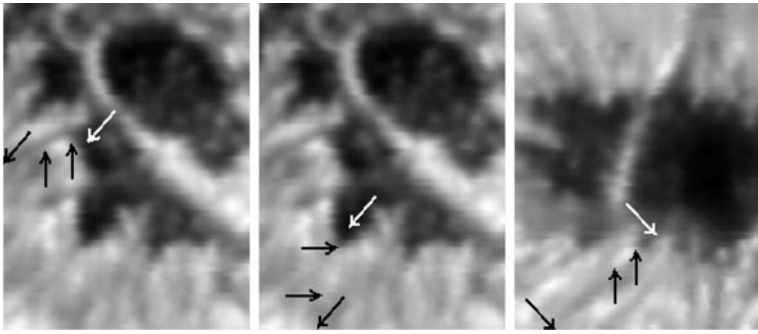


**Figure 4** The maps of continuum intensity with marked position of the vertical cuts through the penumbra. The beginnings and the ends of the cuts are marked with the inclined arrows, which are white and black, respectively. The vertical arrows (cut 1 and 3) and horizontal arrows (cut 2) enclose the bright grains and correspond to the dashed black lines in Figures 5–7.

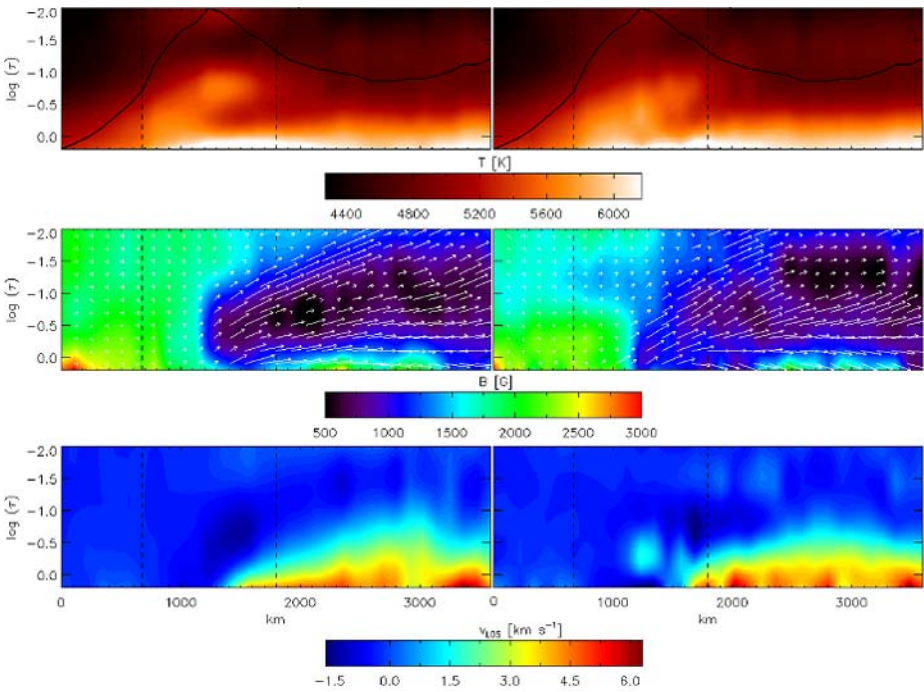


**Figure 5** The stratifications of temperature (upper row), magnetic field strength together with velocities along the field lines marked by the white arrows (middle row), and line-of-sight velocity (lower row) along the vertical cut through the penumbra. The stratifications in the left and right columns correspond to inversions 1 and 2, respectively, with regard to the different setting in the numbers of nodes (see Table 1). The position of the cut in the penumbra is marked on the left map in Figure 4.

becomes horizontal with increasing horizontal distance. The structure is more prominent in this figure than in Figures 6 and 7, because the upper threshold of the temperature scale is set to 6200 K for this purpose. The flux tubes are approximately 500 K hotter than the

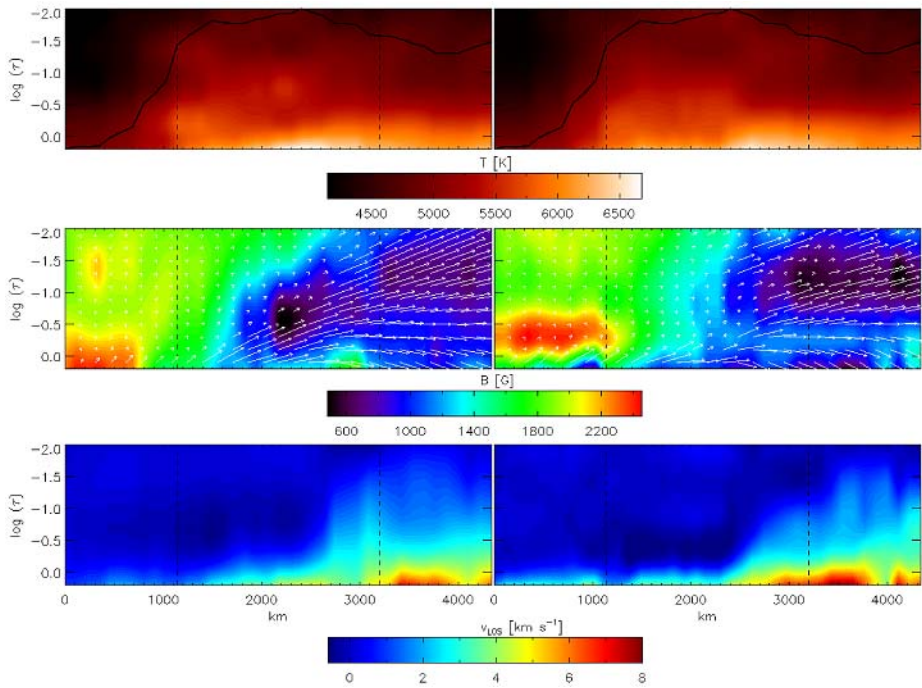


**Figure 6** Same as in Figure 5, but the position of the cut is marked on the middle map in Figure 4.

surrounding plasma close to the point of emergence and 200 K hotter further along the cut. These values can be compared with the azimuthal average of the difference between the background and flux tube components coming from the two-component inversion made by Borrero *et al.* (2006). They found the difference to be around 400 K close to the umbral – penumbral boundary, where the flux tube component is hotter. The temperature difference decreases and the values are comparable around the middle of the penumbra and the background component is hotter than the flux tube component in the outer half of the penumbra. In our case, only parts of the penumbra are observed and thus the position in the penumbra cannot be specified precisely to make a more accurate comparison.

The flux tubes can be clearly seen in the temperature stratifications only close to the point of emergence. However, the cooled parts of the flux tubes can be followed in the plots of magnetic field strength (middle rows in Figures 5–7), as the field is weak inside it. Previous analyses (Bellot Rubio, Balthasar, and Collados, 2004; Borrero *et al.*, 2006) found the biggest difference in magnetic field strength between the background and flux tube component in the inner penumbra (around 500 and 1500 G, respectively) and this difference decreased to zero in the outer parts of the penumbra. We found the magnetic field in the flux tube only slightly decreased (by 200 G) in the area of the bright grain, but the difference increases up to 600 G further.

According to the model, the flux tube should be horizontal further from the bright grain. The orientation of the white arrows in the maps of magnetic field (middle rows in Figures 5–7) corresponds to the inclination of the magnetic field lines. In the left columns it can be seen that the inclination decreases with increasing height in the atmosphere, *i.e.* the field becomes more vertical, and the flux tubes cannot be distinguished. This is caused by



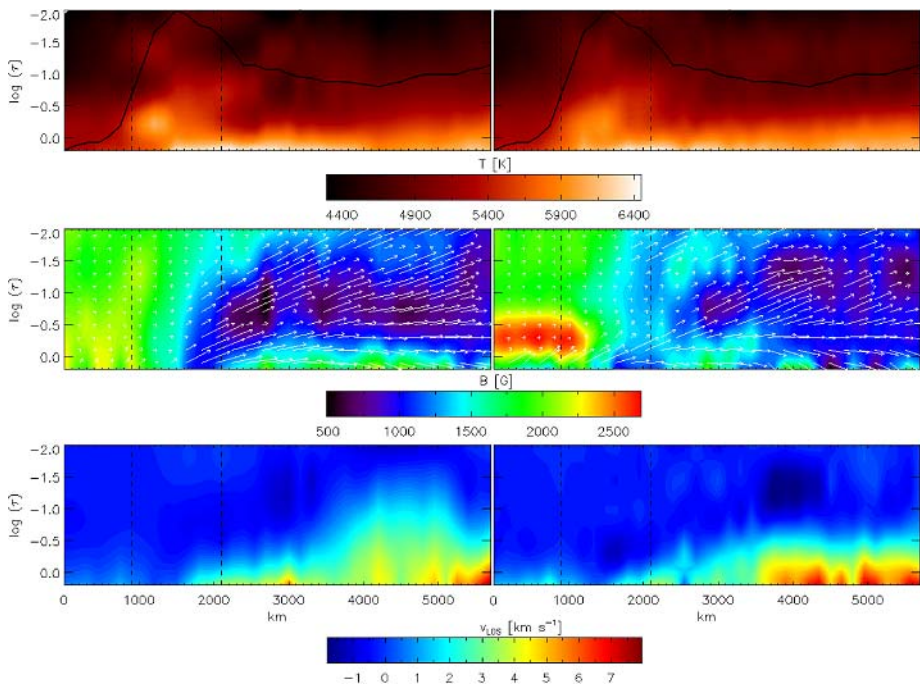


**Figure 7** Same as in Figure 5, but the position of the cut is marked on the right map in Figure 4.

the insufficient number of nodes for the inclination. Having nine nodes for the inclination (right columns) increases the height resolution of the inversion. In this case, the maximal inclinations are still found at the lowest layers, then they decrease with height up to the areas with weak magnetic field, where the inclinations increase to values usually around  $80^\circ$  and decrease again at higher layers.

The two-component inversions made by Bellot Rubio, Balthasar, and Collados (2004) and Borrero *et al.* (2006) show the averaged inclination of the flux tube around  $60^\circ$  close to the umbra, which is comparable with our results in places of the bright grains. The difference is in the values of inclination of the magnetic field in the surrounding penumbra, which is in our case still around  $60^\circ$ , but only  $20^\circ$  in case of two-component inversion.

In the lowest rows in Figures 5–7 can be found the stratifications of the LOS velocity along the cut. The flux tubes cannot be detected in the left columns for the same reason as in the case of inclination, *i.e.* insufficient number of nodes. However, very similar stratifications of the LOS velocity are obtained with the higher number of nodes: There is a smooth decrease with height, and no indication of the flux tubes carrying the Evershed flow can be found at heights with weak and horizontal magnetic field. Therefore, these results cannot be compared with the two-component inversions, where *e.g.* Borrero *et al.* (2006) found LOS velocities around  $3 \text{ km s}^{-1}$  for the flux tube component. However, higher values of the LOS velocity were found at the optical depth  $\log \tau = -1$  than at  $\log \tau = 0$  by Borrero *et al.* (2004) with one-component inversion, a result that supports the location of the flux tubes around this height in the penumbra but is not confirmed by our stratifications.

The theoretical model by Schlichenmaier, Jahn, and Schmidt (1998) predicts upflows in the bright grains and outflows in places where the flux tube is horizontal. In some cases, the

upflows can be seen in the maps of the LOS velocities. For example, on the left map of the LOS velocities in Figure 5 can be seen an area with upflows, but on the right map this area splits into smaller areas with downflows and stronger upflows. However, more significant upflows are obtained with higher number of nodes for the third cut (Figure 7).

By assuming that the orientation of the flow corresponds to the orientation of the magnetic field, the velocities along the field lines can be easily derived from the values of inclination and LOS velocity. For this purpose we assumed that the flow has the same orientation as the cut through the penumbra (*i.e.* as the flux tube) and neglect the obtained values of magnetic field azimuth shown in Figure 3.

The resulting velocities along the magnetic field lines are represented by the white arrows in the maps of magnetic field strength (middle rows in Figures 5–7). The length of the arrows corresponds to the amplitude of the velocity, which is limited to  $10 \text{ km s}^{-1}$ . The problem is that the obtained velocities are rather uncertain in places where the projection angle varies between  $80^\circ$  and  $100^\circ$  as the cosine of this angle is used for the computation of the velocity and the error can exceed 100% in these areas.

For the first cut (Figure 5) the fast flows are not detected in areas with weak magnetic field. The correlation between the weak magnetic field and high velocity along the magnetic field lines is better for the second and third cuts (Figures 6 and 7). Unfortunately, there are only a few other cases where the fast flows are located in areas with weak and horizontal magnetic field; the faster flows are mostly located below these regions.

#### 4. Conclusions

In all bright grains in the analysed parts of the penumbra the constructed maps of temperature and magnetic field strength show the theoretically predicted shape of the rising flux tube, *i.e.* the hot filamentary structures are located in places of the bright grains in the penumbra and the weak magnetic field is found in these bright grains and in the dark areas that can be traced back as the extensions of the bright filaments. Moreover, higher values of inclination are reached at the heights of the weak magnetic field if the higher number of nodes is used. The LOS velocities reach the maximal values at deepest layers with no regard to the used number of nodes and there are no increased LOS velocities at heights where the weak and horizontal magnetic field is obtained. The velocities along the magnetic field lines are highly uncertain and although the maximal values are in some cases higher than the maximal values of the LOS velocity they are only rarely correlated with areas with inclined and weak magnetic field.

With the current spatial resolution (500 km) we cannot observe single flux tubes, but only their conglomerates, so that the presented results of the inversion are influenced by complex unresolved structures. The agreement between the theoretical predictions and obtained stratifications of plasma parameters is nonetheless promising. However, observations with higher spatial resolutions (such as those from the Hinode mission) are needed to resolve whether we really observe rising flux tubes or some fine structures in the background field that are not connected with the Evershed flow.

Although the results are compared only with the model of the rising flux tubes suggested by Schlichenmaier, Jahn, and Schmidt (1998), the stratifications of plasma parameters found here do not exclude the model suggested by Spruit and Scharmer (2006) and Scharmer and Spruit (2006), who proposed the existence of field-free gaps in the penumbra. This would mean weaker and more horizontal magnetic fields observed in deep layers at the locations of the gaps. This model does not explain the origin of the Evershed flow, although

it assumes that the increased velocities would be located at the top of the field-free gaps. This would mean increased LOS velocities at the lower layers, a result supported by the obtained stratifications of this plasma parameter.

**Acknowledgements** This work was supported by the research projects IAA3003404 of the Grant Agency of the Academy of Sciences of the Czech Republic and 205/04/2129 of the Czech Science Foundation.

## References

- Beckers, J.M., Schröter, E.H.: 1969, *Solar Phys.* **10**, 384.
- Bellot Rubio, L.R.: 1999, In: *A User Guide to SIR*.
- Bellot Rubio, L.R., Balthasar, H., Collados, M.: 2004, *Astron. Astrophys.* **427**, 319.
- Bellot Rubio, L.R., Schlichenmaier, R., Tritschler, A.: 2006, *Astron. Astrophys.* **453**, 1117.
- Borrero, J.M., Solanki, S.K., Bellot Rubio, L.R., Lagg, A., Mathew, S.K.: 2004, *Astron. Astrophys.* **422**, 1093.
- Borrero, J.M., Solanki, S.K., Lagg, A., Socas-Navarro, H., Lites, B.: 2006, *Astron. Astrophys.* **450**, 383.
- Jurčák, J.: 2006, *Two dimensional spectropolarimetry of a sunspot*, Doctoral thesis, Charles University, Prague.
- Jurčák, J., Martínez Pillet, V., Sobotka, M.: 2006, *Astron. Astrophys.* **453**, 1079.
- Langhans, K., Scharmer, G.B., Kiselman, D., Löfdahl, M.G., Berger, T.E.: 2005, *Astron. Astrophys.* **436**, 1087.
- Martínez Pillet, V.: 2000, *Astron. Astrophys.* **361**, 734.
- Martínez Pillet, V., Collados, M., Sánchez Almeida, J., et al.: 1999, In: *High Resolution Solar Physics: Theory, Observations, and Techniques, ASP Conf. Ser.*, vol. **183**, p. 264.
- Müller, D.A.N., Schlichenmaier, R., Fritz, G., Beck, C.: 2007, *Astron. Astrophys.* **460**, 925.
- Press, W.H., Flannery, B.P., Teukolsky, S.A.: 1986, *Numerical Recipes. The Art of Scientific Computing*, Cambridge University Press, Cambridge.
- Roupe van der Voort, L.H.M., Löfdahl, M.G., Kiselman, D., Scharmer, G.B.: 2004, *Astron. Astrophys.* **414**, 717.
- Ruiz Cobo, B.: 1998, *Astrophys. Space Sci.* **263**, 331.
- Ruiz Cobo, B., del Toro Iniesta, J.C.: 1992, *Astrophys. J.* **398**, 375.
- Scharmer, G.B., Spruit, H.C.: 2006, *Astron. Astrophys.* **460**, 605.
- Scharmer, G.B., Pettersson, L., Brown, D.S., Rehn, J.: 1985, *Appl. Opt.* **24**, 2558.
- Schlichenmaier, R., Jahn, K., Schmidt, H.U.: 1998, *Astron. Astrophys.* **337**, 897.
- Solanki, S.K.: 2003, *Astron. Astrophys. Rev.* **11**, 153.
- Solanki, S.K., Montavon, C.A.P.: 1993, *Astron. Astrophys.* **275**, 283.
- Spruit, H.C., Scharmer, G.B.: 2006, *Astron. Astrophys.* **447**, 343.
- Westendorp Plaza, C., del Toro Iniesta, J.C., Ruiz Cobo, B., et al.: 1998, *Astrophys. J.* **494**, 453.
- Westendorp Plaza, C., del Toro Iniesta, J.C., Ruiz Cobo, B., et al.: 2001a, *Astrophys. J.* **547**, 1130.
- Westendorp Plaza, C., del Toro Iniesta, J.C., Ruiz Cobo, B., Pillet, V.M.: 2001b, *Astrophys. J.* **547**, 1148.
- Wiehr, E.: 2000, *Solar Phys.* **197**, 227.